Cryo-EM Structures of *Azospirillum brasilense* Glutamate Synthase in Its Oligomeric Assemblies

Paolo Swuec [1,2], Antonio Chaves-Sanjuan [1], Carlo Camilloni [1], Maria Antonietta Vanoni [1] and Martino Bolognesi [1,2]

*1 - **Dipartimento di Bioscienze,** Università degli Studi di Milano, Via Celoria 26, 20133 Milano, Italy*
*2 - **Centro di Ricerca Pediatrica Romeo ed Enrica Invernizzi,** Università degli Studi di Milano, Via Celoria 26, 20133 Milano, Italy*

***Correspondence to Paolo Swuec and Martino Bolognesi:** Dept. Biosciences, University of Milano, Via Celoria, 26, 20133 Milano, Italy. martino.bolognesi@unimi.it.*
https://doi.org/10.1016/j.jmb.2019.08.011
Edited by John Johnson

Abstract

Bacterial NADPH-dependent glutamate synthase (GltS) is a complex iron–sulfur flavoprotein that catalyzes the reductive synthesis of two L-Glu molecules from L-Gln and 2-oxo-glutarate. GltS functional unit hosts an α-subunit (αGltS) and a β-subunit (βGltS) that assemble in different αβ oligomers in solution. Here, we present the cryo-electron microscopy structures of *Azospirillum brasilense* GltS in four different oligomeric states ($\alpha_4\beta_3$, $\alpha_4\beta_4$, $\alpha_6\beta_4$ and $\alpha_6\beta_6$, in the 3.5- to 4.1-Å resolution range). Our study provides a comprehensive GltS model that details the inter-protomeric assemblies and allows unequivocal location of the FAD cofactor and of two electron transfer $[4Fe–4S]^{+1,+2}$ clusters within βGltS.

GltS catalyzes the reductive synthesis of two L-Glu molecules from L-Gln and 2-oxoglutarate (2-OG); together with glutamine synthetase, GltS is essential for ammonia assimilation in microorganisms, plants and lower animals [1]. The reaction requires three coordinated catalytic sites and five different prosthetic groups: incoming NADPH reduces FAD at the NADPH oxidizing site in βGltS (~50 kDa); from reduced FAD electrons flow through two low potential $[4Fe–4S]^{+1,+2}$ clusters (in βGltS), and then through a $[3Fe–4S]^{0,+1}$ cluster to FMN, at the synthase site (both in αGltS, ~150 kDa). Here, 2-OG is converted into 2-iminoglutarate (2-IG) upon addition of ammonia released from L-Gln at the PurF-type glutaminase site, the two sites being connected through an intramolecular tunnel; 2-IG is then reduced to L-Glu by reduced FMN [1].

To shed light on the architecture of *Azospirillum brasilense* GltS and of the catalytic centers, we analyzed the enzyme three-dimensional structure through single-particle cryo-electron microscopy (cryo-EM), following a previous crystallographic characterization of the isolated αGltS subunit [2]. Our analysis focused on the recombinant GltS produced as described [3,4] (Supplementary Fig. 1), previously characterized as an $\alpha_6\beta_6$ assembly (1.2 MDa) through a combined SAXS/cryo-EM and modeling approach, at 9.5 Å resolution [5]. Our cryo-EM analyses (at resolutions in the 3.5- to 4.1-Å range) present two main structural results: (i) we detail variable levels of oligomerization for the GltS αβ assembly (from $\alpha_4\beta_3$ to $\alpha_6\beta_6$), and (ii) we provide a residue-resolution level model of βGltS that allows mapping the FAD coenzyme and two $[4Fe–4S]^{+1,+2}$ clusters, thus describing the full electron transfer chain, from NADPH to 2-IG through the five prosthetic groups.

Inspection of the cryo-EM data shows $\alpha_4\beta_3$, $\alpha_4\beta_4$, $\alpha_6\beta_4$ and $\alpha_6\beta_6$ as the four main GltS oligomeric species present in the vitrified specimen (Fig. 1a and Supplemenatry Fig. 2). In agreement with the reported crystal structure and previous low resolution cryo-EM analysis [2,5], all the observed oligomeric species display pairwise association of αGltS, building tight α-dimers ("pillars" endowed with 2-fold internal symmetry; β chains bind at opposed tips of each pillar) (Fig. 1a–b). Thus, the observed GltS assemblies can be defined as oligomers of $\alpha_2\beta_2$ units (each unit showing an internal 2-fold axis relating two αβ protomers). Notably, at 3.5-Å

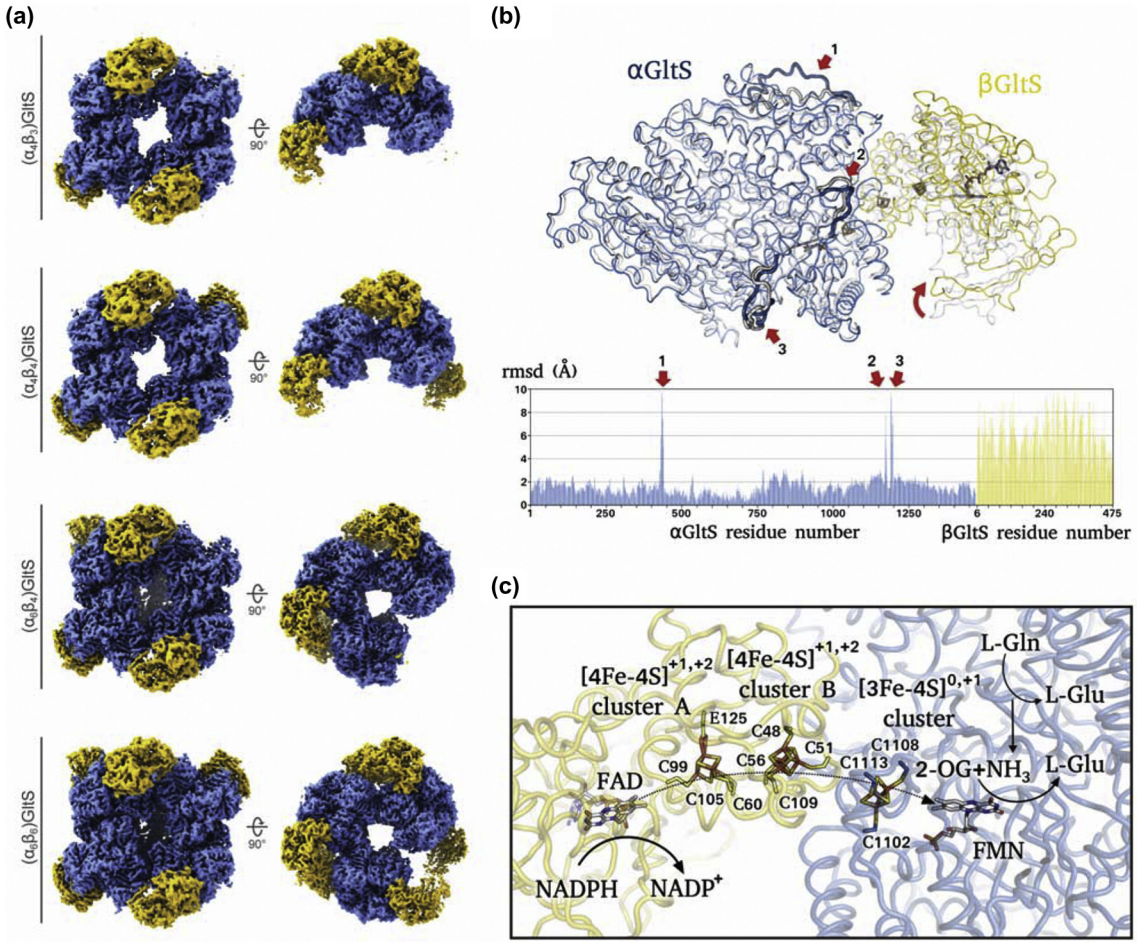

Fig. 1. Architecture of *A. brasilense* GltS oligomeric assemblies revealed by cryo-EM. (a) Orthogonal views of the cryo-EM final 3D reconstructions of the four *A. brasilense* GltS oligomeric assemblies. (b) Comparison of (αβ)GltS atomic models built and refined on high-resolution cryo-EM density maps (color scheme as in panel a) with previously deposited (αβ)GltS models (gray, PDB code 2VDC). The per-residue rmsd between the two structures is reported below. The three main differing regions for αGlts were highlighted and numbered. The shift for βGlts was represented with a red arrow. (c) Detailed view of the FAD-FMN catalytic sites connected by the three Fe/S clusters. The main chain for αGlts and βGlts is represented as semi-transparent ribbon (color scheme as in panel a). Cofactors and side chains for the residues that coordinate Fe/S clusters were represented as sticks and labeled. A schematic representation of the reactions occurring on each catalytic site was included. The electron transfer path was represented as dashed arrow.

resolution, assembly of $\alpha_2\beta_2$ units in the largest observed $\alpha_6\beta_6$ particle [i.e., $(\alpha_2\beta_2)_3$] obeys only marginally internal 32 point symmetry, leaving what appears as a cyclic $\alpha_2\beta_2$ trimer not properly closed due to lose or absent interactions at one of the three expected $\alpha_2\beta_2$ interfaces (Fig. 1a and Supplemenatry Fig. 2]. Lack of $\alpha_2\beta_2$ interaction at this interface is more pronounced in the $\alpha_6\beta_4$ assembly and striking in the lower size species (Fig. 1a). The $\alpha_6\beta_4$ assembly results from loss of two βGltS at the loose contact interface of the $\alpha_6\beta_6$ particle. Subsequent loss of an α-dimer and a further βGltS originates the smaller particles, which nevertheless maintain inter-subunit packing closely matching that of the $\alpha_6\beta_6$ species. Indeed, rmsd values calculated among all Cα atoms building the different assemblies fall in the 0.7- to 0.9-Å range, indicating that association of subunits, even in different ratios, are not reflected by main conformational transitions.

Association of the subunits in the αβ protomer—the functional catalytic unit—relies on an α/β contact area of 1125 $Å^2$ (average over the different oligomers), contributed by 31 βGltS interface residues (5.1% of the total surface area for βGltS). This value should be compared with the α/α (intra-pillar) contact area of 1920 $Å^2$ (average over the different oligomers), contributed by the amidotransferase and FMN binding domains. In addition, each α-subunit displays contacts with a neighboring α-dimer (average 756 $Å^2$ over the different oligomers) through the

first two strands of the extended C-terminal β-helix. The α/β association interface is built by residues in the regions 7−11, 49−84 and 108−116 on βGltS, which contact residues belonging to the 458−463, 678−683, 775−796 and 1103−1127 segments on αGltS. Association of βGltS does not affect the overall αGltS conformation; superposition on the αGltS crystal structure yields an rmsd of 1.2 Å over 1431 Cα atoms, with three localized deviations > 8 Å (Fig. 1b).

The βGltS structure was modeled and fitted to density after a homology model based on the α-subunit structure of NADP(H)-bound NADH-dependent ferredoxin:NADP reductase from *Pyrococcus furiosus* (PDB 5JCA, [6]), as described in Supplemental Material. Manual inspection of the density maps and real space refinement yielded a model close to the previous low resolution βGltS structure [5] for a core region of 330 matched Cα atoms (1.5 Å rmsd), but showing large structural rearrangements in outer regions (rmsd of 4.9 Å for 450 Cα backbone) (Fig. 1b). Of interest are the deviations in the Cys1−Gly52 and Val110−Gly117 regions, involved in contacts with αGltS and close to the [4Fe−4S]$^{+1,+2}$ cluster B. Nevertheless, the FAD binding pocket structure and the location of both low potential [4Fe−4S]$^{+1,+2}$ clusters (A and B) match closely those of the related dehydrogenase models [5,7].

The [4Fe−4S]$^{+1,+2}$ cluster A displays three Cys and one Glu ligands for the Fe atoms (Fig. 1c). Specifically, Cys105 and Cys60 are linked to Fe1 and Fe2, respectively; the Fe3 atom shows bidentate coordination to Glu125 carboxylate; Fe4 is coordinated to Cys99, whose Cα atom falls 5 Å from FAD dimethyl-benzene ring C8 methyl. Conversely, all Cys ligands to the [4Fe−4S]$^{+1,+2}$ cluster B (Cys48, Cys51, Cys56, Cys109) are comprised in βGltS loops at the interface with αGltS.

The FAD coenzyme, the entry site for electrons donated as a hydride anion by NADPH, is fully resolved in the experimental density in all the oligomeric species. The isoalloxazine ring is almost solvent inaccessible (Fig. 1c); neighboring residues are Ile98, Pro100, Leu186, Ile191, Lys195, Leu266, Asp300, Thr301, Asp304, Leu450 and Val451, together with backbone atoms of the surrounding regions. Modeling of the NADPH ligand into βGltS (based on structural homology with NADP(H)-bound NADH-dependent Ferredoxin:NADP reductase from *P. furiosus*, PDB 5JCA, [6]) shows that the cofactor site is properly structured for binding, locating the C4 atom of NADPH nicotinamide ring in the proximity of the isoalloxazine N5 atom.

The observed juxtaposition of the α/β-subunits allows the FAD coenzyme, the Fe/S clusters (in the two subunits) and the electron-receiving FMN cofactor to be all aligned along a slightly bent line (Fig. 1c), at mutual (shortest) distances that vary from 7 Å (FMN C7 methyl group to the S3 atom in the [3Fe−4S]$^{0,+1}$ cluster), to 11 Å (between the [3Fe−4S]$^{0,+1}$ cluster S1 atom and the [4Fe−4S]$^{+1,+2}$ cluster B Fe1 atom), to 10 Å (between S1 atom in cluster B and S4 atom in cluster A), and to 9 Å (between cluster A Fe4 atom and FAD C8 methyl), the two flavin coenzymes being thus located *ca.* 50 Å apart in the assembled αβ protomer. Thus, the GltS structure presented here independently confirms the αβ protomer as the minimal functional unit, fully hosting the linear electron transfer pathway, from FAD to FMN through the low potential [4Fe−4S]$^{+1,+2}$ clusters A and B, and the [3Fe−4S]$^{0,+1}$ cluster in the α-subunit, as opposed to bifurcated pathways previously considered [1,6]. The structural neighborhood of FMN, the ultimate 2-IG reduction site, matches closely that observed at 3.0-Å resolution in the crystal structure of αGltS (PDB 1EA0; [2]). Interestingly, here the cryo-EM maps show extra density at the 2-OG binding site, likely representing a substrate molecule, present in the purification buffers, bound to the enzyme and not released during the final size exclusion chromatography step.

The observed oligomeric species variability, as previously suggested by SAXS and native mass spectrometry data [5,8], highlights an adaptive quaternary assembly and stimulates the search for interactors that may recognize $\alpha_6\beta_6$ GltS or its aggregation sub-species. Our experimental models, in the 3.5- to 4.1-Å resolution range, provide a basis for molecular simulations on inter-subunit communication, coordination of the different GltS activities [9] and analysis of electron transfer pathways and of ligand-based tuning of the Fe/S centers redox potentials.

Accession codes

The cryo-EM maps and the corresponding refined molecular models have been deposited in the Electron Microscopy Data Bank and RCSB Protein Data Bank under the accession codes EMD-10105 and PDB 6S6T for ($\alpha_4\beta_3$)Glts, EMD-10104 and PDB 6S6S for ($\alpha_4\beta_4$)Glts, EMD-10106 and PDB 6S6U for ($\alpha_6\beta_4$)Glts and EMD-10108 and PDB 6S6X for ($\alpha_6\beta_6$) Glts. Other data are available from the corresponding authors upon request.

Acknowledgments

We are grateful to Dr. Delia Tarantino (Dept. Biosciences, U. Milano) for her endless technical

assistance. Sadly, she passed away on August 14; we wish to dedicate this Communication to her memory. Contributions from the University of Milano and Fondazione Romeo and Enrica Invernizzi, to founding and operation of the cryo-EM facility are gratefully acknowledged.

Declaration of Competing Interest

All authors declare no conflicts of interest.

Appendix A. Supplementary data

Supplementary data to this article can be found online at https://doi.org/10.1016/j.jmb.2019.08.011.

Received 5 July 2019;
Received in revised form 13 August 2019;
Accepted 19 August 2019
Available online 29 August 2019

Keywords:
glutamate synthase;
iron/sulfur flavoprotein;
Fe/S clusters;
cryo-electron microscopy;
protein oligomeric structure

Abbreviations used:
GltS, *Azospirillum brasilense* glutamate synthase; αGltS, α-subunit of GltS; βGltS, β-subunit of GltS; rmsd, root mean square deviation; 2-OG, 2-oxoglutarate.

References

[1] M.A. Vanoni, B. Curti, Structure–function studies of glutamate synthases: a class of self-regulated iron-sulfur flavoenzymes essential for nitrogen assimilation, IUBMB Life 60 (2008) 287–300.

[2] C. Binda, R.T. Bossi, S. Wakatsuki, S. Arzt, A. Coda, B. Curti, et al., Cross-talk and ammonia channeling between active centers in the unexpected domain arrangement of glutamate synthase, Structure. 8 (2000) 1299–1308.

[3] H. Stabile, B. Curti, M.A. Vanoni, Functional properties of recombinant Azospirillum brasilense glutamate synthase, a complex iron–sulfur flavoprotein, Eur. J. Biochem. 267 (2000) 2720–2730.

[4] P. Agnelli, L. Dossena, P. Colombi, S. Mulazzi, P. Morandi, G. Tedeschi, et al., The unexpected structural role of glutamate synthase [4Fe–4S](+1,+2) clusters as demonstrated by site-directed mutagenesis of conserved C residues at the N-terminus of the enzyme beta subunit, Arch. Biochem. Biophys. 436 (2005) 355–366.

[5] M. Cottevieille, E. Larquet, S. Jonic, M.V. Petoukhov, G. Caprini, S. Paravisi, et al., The subnanometer resolution structure of the glutamate synthase 1.2-MDa hexamer by cryoelectron microscopy and its oligomerization behavior in solution: functional implications, J. Biol. Chem. 283 (2008) 8237–8249.

[6] C.E. Lubner, D.P. Jennings, D.W. Mulder, G.J. Schut, O.A. Zadvornyy, J.P. Hoben, et al., Mechanistic insights into energy conservation by flavin-based electron bifurcation, Nat. Chem. Biol. 13 (2017) 655–659.

[7] D. Dobritzsch, S. Ricagno, G. Schneider, K.D. Schnackerz, Y. Lindqvist, Crystal structure of the productive ternary complex of dihydropyrimidine dehydrogenase with NADPH and 5-iodouracil. Implications for mechanism of inhibition and electron transfer, J Biol Chem. 277 (2002) 13155–13166.

[8] B. van Breukelen, A. Barendregt, A.J. Heck, R.H. van den Heuvel, Resolving stoichiometries and oligomeric states of glutamate synthase protein complexes with curve fitting and simulation of electrospray mass spectra, Rapid Commun. Mass Spectrom. 20 (2006) 2490–2496.

[9] M.A. Vanoni, B. Curti, Structure–function studies on the iron–sulfur flavoenzyme glutamate synthase: an unexpectedly complex self-regulated enzyme, Arch. Biochem. Biophys. 433 (2005) 193–211.